JOURNAL OF PROPULSION AND POWER
Vol. 14, No. 6, November–December 1998

Effects of Unmixedness in Piloted-Lean Premixed Gas-Turbine Combustors

J. C. Barnes* and A. M. Mellor†
Vanderbilt University, Nashville, Tennessee 37235

The characteristic time model (CTM) represents the dominant physical processes related to combustor performance in terms of characteristic times. Properly formulated, these characteristic times will correlate effects of variations in combustor geometry, fuel characteristics, and operating conditions. Here, a CTM for NO_x emissions is used to investigate the sensitivity of NO formation in piloted-lean premixed combustor to fuel/air unmixedness. The CTM analysis presented here also suggests an experimental method of evaluating premixed performance under fired conditions that is discussed in a companion paper.

Nomenclature

C, $\bar{c}$ = time mean fuel mole fraction measured at a point in the premixer exit plane
C_{av} = fuel mole fraction computed assuming perfect premixing of the main fuel and airflows
CO = carbon monoxide
d_{cb} = diameter of the centerbody, m
$f/a|_{st}$ = stoichiometric molar fuel to air ratio
l_{lip} = ignition perimeter, total circumference for flameholding at premixer exit plane, m
l_{no} = characteristic length for thermal NO formation, m
m = slope of a linear equation
$\dot{m}_a$ = total combustor airflow rate, kg/s
$\dot{m}_{a,\phi=1}$ = effective airflow to the pilot flame in the primary zone, kg/s
NO = nitric oxide
NO_x = oxides of nitrogen, NO and NO_2
NO_xEI = oxides of nitrogen emissions index, g NO_2/kg fuel
NO_2 = nitrogen dioxide
n = pressure exponent
p = pressure, atm
r = correlation coefficient
s = standard deviation in equivalence ratio about $\bar{\phi}_m$ divided by $\bar{\phi}_m$
T = temperature, K
T_{in} = inlet temperature of combustor airflow, K
$T_{\phi,m}$ = adiabatic flame temperature at the main equivalence ratio ($\bar{\phi}_m$), K
$T_{\phi=1}$ = adiabatic stoichiometric flame temperature, K
V_{lip} = cold-flow velocity of the fuel/air mixture at flameholder/premixer exit, m/s
V_{ref} = reference velocity, velocity computed based on $\dot{m}_a$, p_{in}, T_{in}, and the maximum combustor diameter, m/s
$V_{\phi=1}$ = stoichiometric flame zone velocity, m/s
$y_{f,m}$ = mass fraction of total fuel flow to main injector
θ = swirl angle
ρ = density, kg/m^3
σ_c = standard deviation in fuel concentration about C_{av}
σ_y = standard deviation of the y values for the observed x values
σ_ϕ = standard deviation in equivalence ratio about $\bar{\phi}_m$
τ_{no} = characteristic kinetic time for thermal NO formation, ms
τ_{res} = combustor residence time based on reference velocity, ms
$\tau_{sl,no}$ = characteristic fluid time for thermal NO formation, ms
$\tau_{sl,tno}$ = characteristic fluid time for total NO formation, ms
τ_{tno} = characteristic kinetic time for total NO formation, ms
ϕ = overall combustor equivalence ratio based on total air and fuel flow rates
ϕ_{eddy} = local equivalence ratio of a single eddy
$\bar{\phi}_m$ = equivalence ratio computed assuming perfect premixing of the main fuel and airflow
$\Psi(\phi_{eddy})$ = probability density function corresponding to a time-averaged spatial distribution in equivalence ratio in a lean-premixed flame

Subscripts
a = air
eddy = single reacting eddy
f = fuel
in = inlet value
m = flow through the main injector, i.e., the premixer
$\phi < 1$ = lean premixed flame
$\phi = 1$ = pilot diffusion flame

Introduction

LEAN-PREMIXED (LP) combustion is a technique for pollutant emissions control that is seeing increased application in gas turbines as an alternative to conventional, diffusion flame combustion. The LP combustor is distinctly different from the diffusion-flame combustor in that a significant portion of the combustor air is mixed with fuel upstream of the primary zone. In the low-emissions mode, a combustor of this type ideally produces a homogeneous lean fuel and air mixture and thereby eliminates the stoichiometric eddies found in conventional, diffusion flame combustors. Premixing thus allows for greater control of local equivalence ratios so that Zeldovich NO (also called thermal NO), which becomes significant at temperatures greater than approximately 1800 K, can be minimized. Similarly, by maintaining sufficient combustor residence times at temperatures between 1300 and 1700 K, final CO levels are negligible if local quenching is avoided. However, the fuel and air are not usually perfectly premixed

Received July 11, 1997; revision received March 2, 1998; accepted for publication April 23, 1998. Copyright © 1998 by J. C. Barnes and A. M. Mellor. Published by the American Institute of Aeronautics and Astronautics, Inc., with permission.

*Graduate Research Assistant, Department of Mechanical Engineering; currently Analyst, Enron International, P.O. Box 1188, Houston, TX 77251-1188.

†Centennial Professor of Mechanical Engineering. Associate Fellow AIAA.

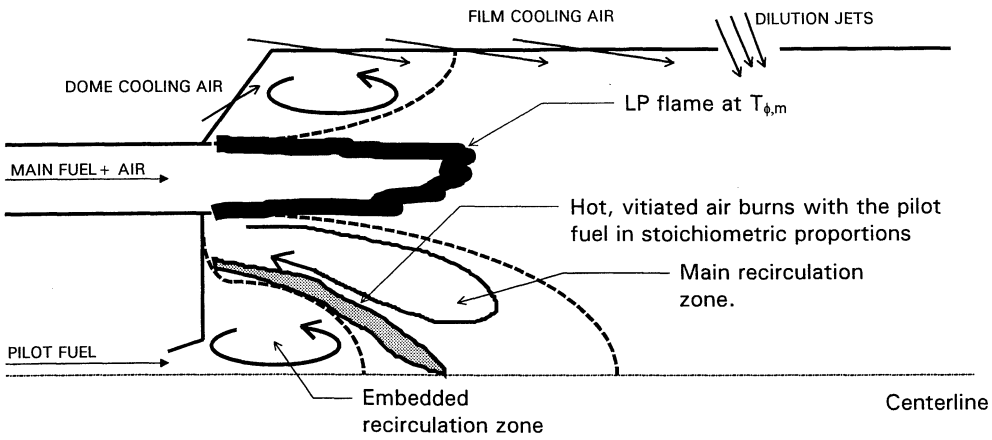

Fig. 1 Schematic of a generic piloted-LP combustor operating in the piloted-LP mode. The pilot fuel burns with the hot, vitiated products of the main flame in stoichiometric proportions.

in LP combustors. Therefore, emissions from LP combustors are not as low as perfectly premixed flameholder results documented in the literature indicate they could be.

To investigate NO formation in advanced gas-turbine combustors, Barnes et al.[1] collected experimental data from an industrial, natural gas-fired, can combustor rig. This combustor is referred to here as "combustor A" and operates in a stable, low-emissions mode at full power. However, a pilot (diffusion) flame is required to maintain combustion at low load conditions. Thus, combustor A is termed a piloted-LP combustor. A schematic of a generic piloted-LP combustor is shown in Fig. 1.

In the combustor A tests, independent variations of equivalence ratio, inlet pressure (8–14 atm), inlet temperature (550–750 K), and residence time (13 and 23 ms) were performed. Barnes et al. used these data to develop a preliminary characteristic time model (CTM) for NO_x emissions from piloted-LP combustors. The CTM for gas-turbine combustor emissions assigns characteristic times, which are based on combustor geometry, fuel characteristics, and operating conditions, to the dominant processes of combustion related to performance and pollutant emissions. Linear ratios of these characteristic times, or of sums of the times weighted with empirical constants, describe the emissions index of NO_x. Here, after a brief summary of the piloted-LP NO_x CTM, the model is used to investigate the sensitivity of NO formation in piloted-LP combustors to fuel/air unmixedness, of necessity measured under cold-flow conditions. Barnes and Mellor[2] discuss some of the difficulties associated with measurements during combustor firing and suggest an alternate method based on exhaust plane determinations of CO emissions.

Characteristic Time Model for Piloted-Lean Premixed NO_x Emissions

The NO_x model for a staged (piloted-LP) combustor must include terms that account for NO formed in both the LP and pilot diffusion flames. In applying the CTM to the pilot flame, it is assumed, following Tuttle et al.,[3] that diffusion flame NO_x emissions index (g NO_2/kg fuel) is proportional to a Damköhler number (the ratio of a fluid mechanic time to a chemical kinetic time):

$$NO_xEI|_{\phi=1} = 4.41(1 - y_{f,m})(\tau_{sl,no}/\tau_{no}) \pm 1.02 \qquad (1)$$

Here, $\tau_{sl,no}$ is the characteristic fluid mechanic time for stoichiometric eddy dissipation and τ_{no} is the characteristic kinetic time for thermal NO formation, both in the postflame region. The subscript $\phi = 1$ denotes the pilot diffusion flame, and the correlation slope and standard deviation are from Newburry and Mellor.[4] The mass fraction of the total combustor fuel flow to the pilot flame $(1 - y_{f,m})$ is included to account for the fact that the number of stoichiometric eddies varies with the mass flow of fuel to the pilot flame.

Tuttle et al.[3] defined the kinetic time as

$$\tau_{no} = 10^{-12} \exp(67{,}976/T_{\phi=1}) \qquad (2)$$

where the pre-exponential factor, in milliseconds, is selected such that the characteristic time ratio in Eq. (1) is on the order of unity. The global activation temperature (67,976 K) for diffusion flame NO formation was deduced empirically from Arrhenius graphs and, following Tuttle et al.,[5] the appropriate temperature associated with the NO-forming eddies is the stoichiometric adiabatic flame temperature, also denoted by subscript $\phi = 1$. Note that in a piloted-LP combustor having the configuration shown in Fig. 1 and operating with both pilot and main fired, the former is supplied with hot, vitiated air from the LP flame. Therefore, the stoichiometric flame temperature must be modified to account for inlet air vitiation and preheating effects.

The characteristic fluid mechanic time is defined as[6]

$$\tau_{sl,no} = l_{no}/V_{\phi=1} \qquad (3)$$

where the stoichiometric flame zone velocity is used to estimate the velocity of stoichiometric eddies convecting through the combustor

$$V_{\phi=1} = (\dot{m}_{a,\phi=1}/\dot{m}_a)(T_{\phi=1}/T_{in})V_{ref} \qquad (4)$$

The ratio of airflow rates accounts for the mass fraction of combustor airflow that accelerates the stoichiometric eddies through the primary zone,[6] and V_{ref} is the combustor reference velocity based on combustor cross-sectional area.

For the pilot flame in combustor A, the length scale associated with thermal NO formation was defined by Barnes et al.[1] as

$$l_{no}^{-1} = (d_{cb}/\cos\,\theta)^{-1} + d_{cb}^{-1} \qquad (5)$$

This modification of Mellor and Washam's l_{no} accounts for the d_{cb} determining the radial and axial extent of the centerline recirculation zone; the cosine of the swirl angle θ models the augmentation of streamline lengths through the combustor primary zone caused by swirl.[6] The mass flow ratio in Eq. (4) was then arbitrarily set equal to 0.25 for combustor A so that the slope in Eq. (1) applies to the pilot in this preliminary model.

Subsequent analysis of the flow in combustor A has been performed by Hamer and Roby‡ using STAR–CD. Reacting

‡Hamer, A. J., and Roby, R. J., Hughes Associates, Inc., Personal Communication, 1995 and 1996.

flow was simulated using a three-step methane mechanism provided by Nicol and Malte§ and a somewhat coarse mesh. Four cases were considered in which $y_{f,m}$ was varied first, from 1.0 to 0.5, and for the latter fuel split overall ϕ and combustor pressure were then changed independently. The air swirler in the premixing passage, not shown in Fig. 1, was also modeled.

Results indicate that the flow pattern suggested by Fig. 1, Eq. (5), and the corresponding mass flow ratio of 0.25 are incorrect. The swirl at the exit of the premixing passage is sufficiently strong that for $y_{f,m} = 1.0$ the recirculation pattern fills the primary zone (as in a conventional combustor). As $y_{f,m}$ is decreased to 0.5, a strong pilot jet flows along the combustor axis and disrupts the recirculation zone. An annular double-vortex pattern results, as found for flows without swirl by Lightman and Magill[7] and Roquemore and Britton.[8] The flow from the premixing passage follows the outer shear layer surrounding the recirculation zone, but the entrainment of premixer effluent is predicted to decrease by a factor of approximately 3 when $y_{f,m}$ equals 0.5 based on computed tracer gas concentration contours.

These observations will require modification of Eq. (5). The STAR–CD estimates of mass flow will be compared with those resulting from the methodology of Mellor and Washam,[6] as will the length scale associated with pilot NO formation. However, it is anticipated that any resulting change in the slope of 4.41 in Eq. (1) will be negligible; therefore, in the following text the preliminary model of Barnes et al.[1] will be utilized.

This model demonstrates that when combustor A operates in the piloted-LP mode, thermal NO production in stoichiometric eddies originating in the pilot flame region comprises the dominant fraction of total NO production for $y_{f,m}$ less than approximately 0.70. Barnes et al. correlated pilot-dominated combustor A NO_x data with a standard deviation of approximately ± 11 ppmvd (parts per million by volume, dry), 15% O_2.

The following global expression was assumed for the LP flame:

$$\mathrm{NO}_x\mathrm{EI}|_{\phi<1} = y_{f,m} m|_{\phi<1} (\tau_{sl,\mathrm{no}}/\tau_{\mathrm{no}}) \tag{6}$$

where m is a best-fit slope based on regression analysis. The appropriate fluid mechanic time ($\tau_{sl,\mathrm{no}}$) is computed following Magruder et al.[9]

$$\tau_{sl,\mathrm{no}} = l_{\mathrm{lip}}/V_{\mathrm{lip}} \tag{7}$$

In Eq. (7) V_{lip} is the axial cold-flow velocity of the fuel/air mixture at the flameholder/premixer exit plane, and l_{lip} is the ignition perimeter, defined as the total circumferential length around the open fuel/airflow path through the flameholder exit plane (l_{lip} characterizes the anchored flame base length at the flameholder lip that is one factor that determines the surface area of the LP flame; V_{lip} characterizes the velocity of the fuel/air mixture through the LP flame zone).

Following Nicol[10] the chemical kinetic time for LP NO formation (τ_{no}) is (again in milliseconds)

$$\tau_{t\mathrm{no}} = \exp(A) \cdot T_{\mathrm{in}}^{(B+CT_{\phi,m}+Dp_{\mathrm{in}})} \cdot p_{\mathrm{in}}^{(E+FT_{\phi,m}+GT_{\mathrm{in}})} \cdot \exp\left(\frac{H + Ip_{\mathrm{in}} + JT_{\mathrm{in}}}{T_{\phi,m}}\right) \tag{8}$$

where A through J are empirical constants. The appropriate constants for Eqs. (6) and (8) can be computed by performing multiple variable regression analysis for a given set of LP NO_x data. Barnes et al.[1] correlated the combustor A NO_x data for which $y_{f,m}$ was one, i.e., the pure LP data, with either Eq. (8) or a similar equation with $D = G = I = 0$ and obtained a standard deviation of ± 6 ppmvd, 15% O_2. Barnes[11] found the slope in Eq. (6) to be 4.43. Omitting Eq. (7) from the correlation significantly increased the standard deviation.

§Nicol, D. G., and Malte, P. C., University of Washington, Personal Communication to R. J. Roby, Hughes Associates, Inc., 1996.

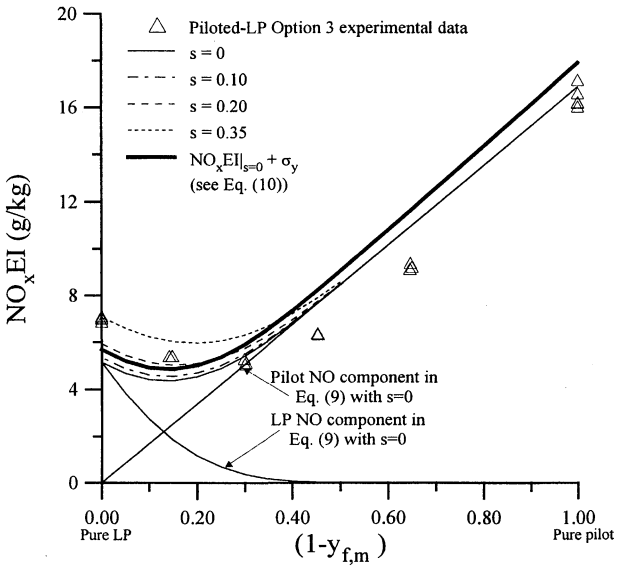

Fig. 2 Total NO_x prediction vs $1 - y_{f,m}$ for unmixedness parameter $s = 0$ using Eq. (9). The individual pilot and LP NO components in Eq. (9) are shown for the $s = 0$ case. Total NO_x predictions for $s > 0$ use Eq. (18). Experimental data[1] are shown for the same combustor operating conditions.

Equations (1) and (6) are summed to model the combustor A piloted-LP NO_x emissions[12]

$$\mathrm{NO}_x\mathrm{EI} = 4.41(1 - y_{f,m}) \frac{\tau_{sl,\mathrm{no}}}{\tau_{\mathrm{no}}} + 4.43 y_{f,m} \frac{\tau_{sl,t\mathrm{no}}}{\tau_{t\mathrm{no}}} \tag{9}$$

The standard deviations of the pilot NO_x and the LP NO_x model were noted in the previous text. The standard deviation associated with the piloted-LP model is a function of $y_{f,m}$, i.e., the relative magnitudes of the modes of NO production

$$\sigma_y^2 = [(1 - y_{f,m})\sigma_y|_{\phi=1}]^2 + [y_{f,m}\sigma_y|_{\phi<1}]^2 \tag{10}$$

Figure 2 shows the model prediction of total NO_xEI as a function of $(1 - y_{f,m})$; the curves with unmixedness parameter $s \neq 0$ will be discussed later. Note that a nonlinear trend in the data near $y_{f,m} = 1$ is predicted by the fuel-mass-fraction-weighted sum of the pilot and LP NO_x correlations and is consistent with that in the Barnes et al.[1] experimental data. The exponential decrease in LP flame NO with a linear increase in pilot flame NO may yield, over a certain range of $y_{f,m}$, a net decrease in total NO.

In Eq. (9) it is assumed that the total amount of pilot NO forms through the thermal mechanism at a rate that is a function of the stoichiometric flame temperature. The consistency of the results of Newburry and Mellor[4] and Mellor and Washam[6] supports this assumption. However, with respect to the LP NO component in Eq. (9), it is likely that spatial and temporal concentration gradients (unmixedness) in the fuel/air mixture at the premixer exit lead to a distribution in LP NO formation rates. Nevertheless, for the preliminary model discussed earlier, unmixedness was ignored. Barnes et al.[1] correlated all of the combustor A NO_x data using Eq. (9), as shown in Fig. 3, with a standard deviation of ± 11 ppmvd, 15% O_2.

Effect of Unmixedness on Lean Premixed NO_x Emissions

Razdan et al.[13] measured the performance of two premixer configurations. In configuration 1, fuel flows through oval-shaped fuel tubes that project radially inward from the fuel

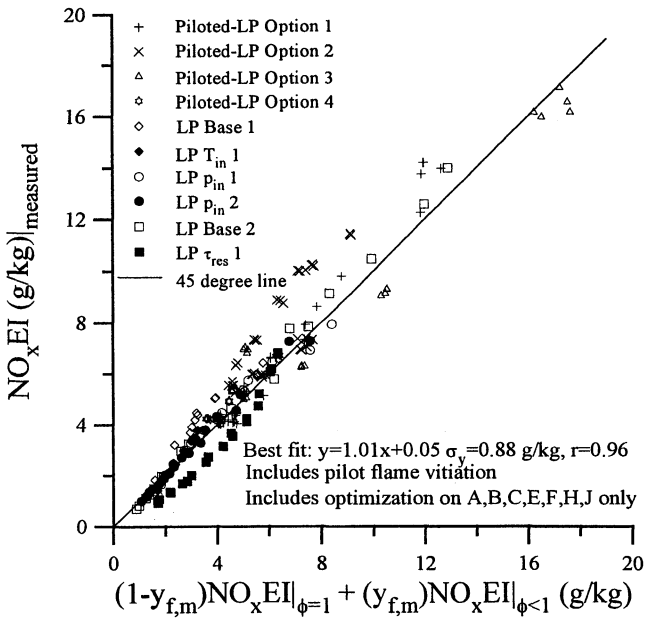

Fig. 3 Preliminary correlation of combustor A NO_x data. Agreement is approximately ±11 ppmvd, 15% O_2. 8 ≤ p_{in} ≤ 14 atm, 550 ≤ T_{in} ≤ 750 K, τ_{res} = 13 or 23 ms, 0.5 ≤ ϕ ≤ 0.8, and 0 ≤ $y_{f,m}$ ≤ 1.

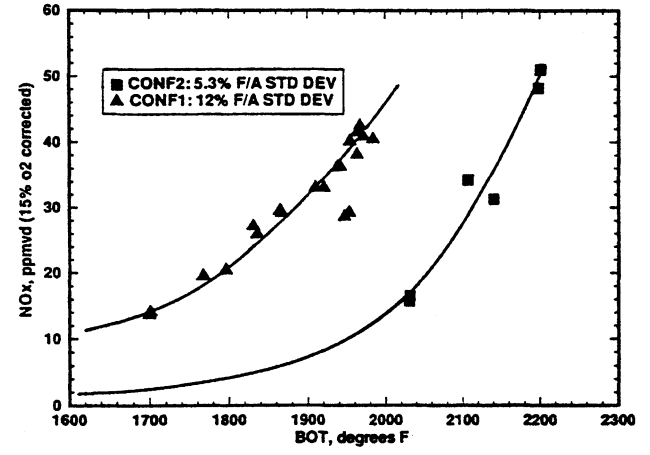

Fig. 4 Comparison of NO_x emissions using two premixer configurations. Results indicate a significant increase in NO_x emissions using configuration 1, which has the higher fuel/air standard deviation. Burner outlet temperature (BOT), was calculated from the measured fuel and airflow rates.[13]

manifold. Fuel is distributed into the premixer air through six small holes in each fuel tube. The fuel and air then flow through a curved vane axial swirler. Configuration 2 was designed to improve upon the mixing characteristics of configuration 1. The axial swirler has 12 hollow airfoil-shaped vanes through which fuel is distributed to small holes on each vane's leading edge. The number of fuel injection holes was increased over that in configuration 1 to approximately 12 on each vane.

Both premixer configurations were tested in an atmospheric pressure, cold-flow rig. In these tests a tracer gas consisting of a known mixture of natural gas and air was injected through the fuel holes, and local samples of fuel/air mixture were collected with a traversing probe. The measured local mole fraction, C, of tracer gas was normalized by the mole fraction computed assuming perfect premixing of the total metered fuel/airflow through the premixer cup, C_{av}. Measurements were made at various radii and azimuthal positions in the premixer exit plane. The standard deviation in the fuel/air measurements for configuration 1 was about 12% of C_{av}, whereas for configuration 2 it was about 5.5% of C_{av} (perfect premixing would correspond to a standard deviation of zero). Razdan et al.[13] indicate significant discrepancies between the NO_x levels from the two configurations as shown in Fig. 4. As expected, the increase in NO_x between the two configurations correlates with the corresponding increase in unmixedness.

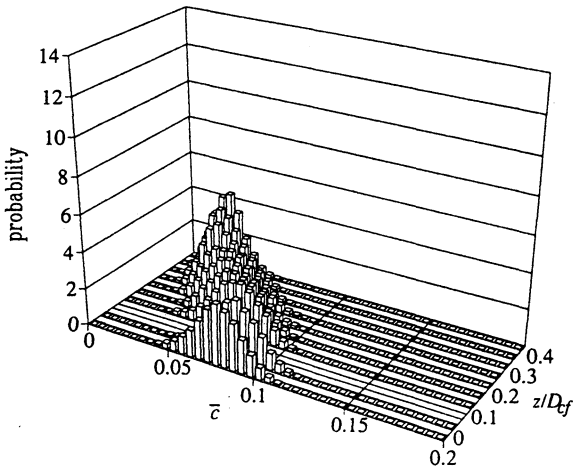

Fig. 5 For $\bar{c}$, the time-averaged fuel concentration computed at each point in the premixer exit plane, and D_{cf} the diameter of the coflow, example PDFs obtained at increasing radii (z) are shown. The fuel concentration assuming perfect premixing of the mean fuel and airflow rates is 0.05.[16]

Fric[14] used the NO_2 LIF technique of Gulati and Warren[15] to measure cold-flow fuel/air mixing at atmospheric pressure. The combustor is located inside a suction wind tunnel. The fuel and air are supplied axially through concentric jets upstream of the flameholder. The premixer and combustor sections were made of quartz to allow optical access to the flame. As in the Razdan et al. tests, mixedness measurements were made under cold-flow conditions and later compared to relative changes in NO_x emissions observed under fired conditions. Mixedness was varied by changing the distance from the jet exit to the flameholder and/or by diverting some air from the coflow to the fuel jet (where all air to the coflow and all fuel to the jet would yield the highest unmixedness at the exit plane of the premixer for a given jet origin). LIF measurements along lines of constant vertical height were sampled at a rate of approximately 20 kHz; thus, spatial and temporal variations in local fuel/air concentration can be measured.

Consistent with the findings of Razdan et al., Fric shows significant increases in NO_x because of spatial unmixedness (on the order of 200% and greater). Also, by holding the time-mean local fuel concentration constant and varying the rms concentration, Fric was able to demonstrate that temporal unmixedness of 10% yields NO_x increases on the order of 100%. Finally, Fric computed fuel concentration probability density functions (PDFs) like those shown in Fig. 5 for each vertical height, z, in each of his test cases.

Model Modified to Account for Unmixedness Effects

If the main fuel and air mixture is not homogeneous, then a distribution of equivalence ratios exists in the LP flame (Fig. 5). Following Mikus and Heywood[16] and Fletcher and Heywood,[17] it is assumed that this equivalence ratio distribution is Gaussian and is centered about the equivalence ratio computed assuming perfect premixing of the main fuel and air. Therefore, the form of the PDF for eddies in the LP flame, for time-averaged standard deviation in equivalence ratio, denoted σ_ϕ, is

$$\Psi(\phi_{\text{eddy}}) = \frac{1}{\sigma_\phi\sqrt{2\pi}} \exp\left[\frac{-(\phi_{\text{eddy}} - \bar{\phi}_m)^2}{2\sigma_\phi^2}\right] \qquad (11)$$

A standard deviation of zero corresponds to the perfectly pre-

mixed case in which all eddies in the LP flame burn with an equivalence ratio equal to the mean.

Alternatively unmixedness can be expressed as a fraction of the equivalence ratio computed assuming perfect premixing. Following Mikus and Heywood this parameter is defined as follows:

$$s \equiv \sigma_\phi / \bar{\phi}_m \tag{12}$$

Using Eq. (12) in Eq. (11) one has

$$\Psi(\phi_{\text{eddy}}) = \frac{1}{s\bar{\phi}_m\sqrt{2\pi}} \exp\left[\frac{-(\phi_{\text{eddy}}/\bar{\phi}_m - 1)^2}{2s^2}\right] \tag{13}$$

A graph of $\Psi(\phi_{\text{eddy}})$ for s equal to 0.2 and $\bar{\phi}_m$ to 0.6 is shown in Fig. 6. It is noted that individual eddy equivalence ratios (ϕ_{eddy}) that are greater than the mean lead to increased NO_x emissions via the exponential decrease in the NO formation time with increasing eddy flame temperature [Eq. (8)].

Before qualitative comparisons can be made between Eqs. (11) and (13) and experimental data, however, a subtle difference between unmixedness measurements and the preceding unmixedness model should be pointed out. Unmixedness is deduced from local fuel concentration measurements taken in the unburned fuel/air mixture upstream of the LP flame. These local measurements are usually reported in terms of C. The magnitude of the standard deviation in the local fuel mole fraction (σ_c) with respect to the fuel mole fraction computed assuming perfect premixing of the main fuel and air, C_{av}, is a common definition of unmixedness, as discussed previously. Equation (12) is based on this concept; however, Eq. (12) is written in terms of the equivalence ratio computed assuming perfect premixing and the standard deviation in local equivalence ratio.

The conversion between fuel mass fraction and equivalence ratio in a premixed, nonreacting fuel/air mixture is

$$\phi = C/(1 - C)(f/a|_{\text{st}}) \tag{14}$$

Expanding the right-hand side of Eq. (14) in a power series and ignoring nonlinear terms one has for $\phi << 1$

$$\phi \approx C/(f/a|_{\text{st}}) \tag{15}$$

Because reasonable agreement between Eqs. (14) and (15) can be expected only for very lean combustor equivalence ratios, and not the region of interest ($\phi = 0.5$–0.6), direct comparisons between the ϕ PDF model and measurements must be treated with caution, particularly if a large fraction of local equivalence ratios much greater than one exists in the sampling region, e.g., near the fuel injector, far upstream of the premixer exit plane. Nevertheless, using Eq. (15)

$$\sigma_\phi \approx \sigma_c/(f/a|_{\text{st}}) \tag{16}$$

and thus

$$s = \sigma_\phi/\bar{\phi}_m \approx \sigma_c/C_{\text{av}} \tag{17}$$

By Eq. (17) standard deviations based on σ_c and C_{av} are only approximately equal to s.

Comparisons between the unmixedness model and experimental measurements can now be made to address the validity of the Gaussian equivalence ratio PDF used in Eqs. (11) and (13). For example, a histogram of the local fuel concentration measurements of Razdan et al.[13] can be fit as Gaussian, with r of the best-fit 0.97. The high correlation coefficient indicates that the Gaussian distribution function is an appropriate assumption for the mole fraction data of Razdan et al. As noted earlier, because the distribution in mole fraction is approximately Gaussian, the distribution in equivalence ratio is Gaussian as well.

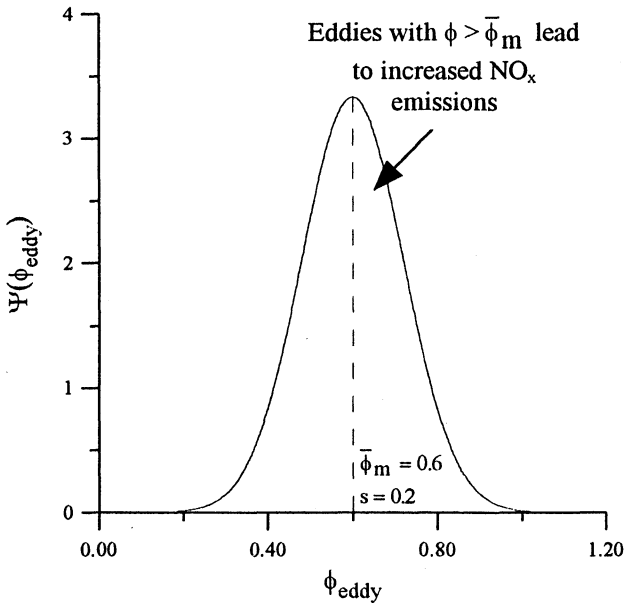

Fig. 6 Graph of Eq. (13) with $\bar{\phi}_m = 0.6$ and $s = 0.20$.

The fuel/air mole fraction PDFs reported by Fric[14] (see Fig. 5) appear to be Gaussian also. However, note that because Eq. (13) characterizes equivalence ratio distribution at a given axial station, it is the distribution associated with the entire ensemble of measurements shown in Fig. 5 that should be compared to Eq. (13). Such results were not reported by Fric. However, Mongia et al.[18] report Gaussian fuel mole fraction PDFs for various axial planes in a coaxial premixer that is similar to that used by Fric.

Finally, the assumed Gaussian PDF can be compared to the computed fuel/air mixing results,‡ where STAR–CD was also used to investigate fuel/air mixing downstream of the fuel injector designed for the tests discussed by McDonald and Mellor.[19] Fuel travels through a single center manifold and is distributed through holes angled 45 deg upstream in each of the fuel pegs. Airflow is unswirled and perpendicular to the fuel spokes. Based on the experimental unmixedness results discussed earlier, one would expect time-averaged PDFs in equivalence ratio to become more Gaussian with increasing downstream distance. Gaussian best-fits of the equivalence ratio histograms for axial stations two and four pipe diameters downstream of the premixer are shown in Fig. 7. As indicated by the low correlation coefficients, the agreement between the Gaussian best-fit and the predicted equivalence ratio distribution is poor, although improving with downstream distance. However, note that discrepancies between experimental measurements and computational fluid dynamics (CFD) predictions of unmixedness were reported by Hautman and co-workers,[20,21] and Snyder et al.[22] Specifically, Hautman and coworkers found that CFD overpredicted the observed mixing rate in their studies, so that local values of s deduced from CFD, as in Fig. 7, should be considered too low.

Applying Eq. (13) to Eq. (9) one has

$$\text{NO}_x\text{EI}|_s = 4.41(1 - y_{f,m})\frac{\tau_{sl,\text{no}}}{\tau_{\text{no}}} + 4.43y_{f,m}\int_0^{1.4} \frac{\Psi(\phi_{\text{eddy}})\tau_{sl,\text{no}}}{\tau_{\text{no}}(\phi_{\text{eddy}})}\,\text{d}\phi_{\text{eddy}} \tag{18}$$

The integrand represents NO formation in an individual eddy in the LP flame with an equivalence ratio of ϕ_{eddy}. Equation (18) reduces to Eq. (9) as s approaches zero. The lower integration limit is selected to match the lower limit of equivalence ratio, and for nominal combustor operating conditions, the up-

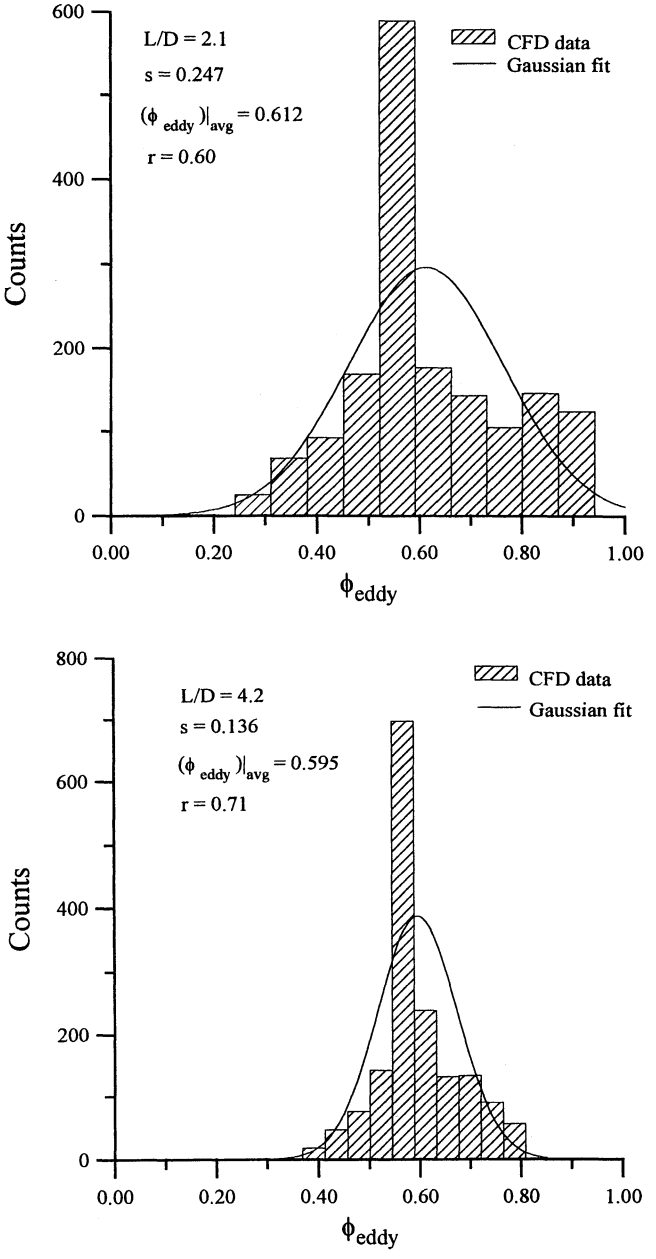

Fig. 7 Gaussian best-fit to the predicted equivalence ratio distribution at two and four premixer diameters downstream.

per integration limit of 1.4 is sufficient to capture more than 99% of the integral over the range $\pm\infty$ (Fig. 8).

Recall that the LP NO component in Eq. (18) was calibrated by Barnes et al.[1] for equivalence ratios between approximately 0.5 and 0.8. Therefore, the LP model is extrapolated for ϕ_{eddy} outside of this range. The total LP NO formation model in Eq. (18) should apply with negligible error to eddies with ϕ_{eddy} less than 0.80 (where nonthermal NO formation is most significant). Because the kinetic time associated with eddies with ϕ_{eddy} approaching one is more appropriately modeled by τ_{no}, some error is expected with the extrapolation of the total LP NO model in Eq. (18) for ϕ_{eddy} beyond 0.80. Nevertheless, in the preliminary analysis presented here, this error is expected to be second order with respect to the value of the Eq. (18) integral over all NO-forming eddies. Possible errors of this type can be more appropriately evaluated when simultaneous NO_x and unmixedness measurements become available.

The ϕ PDF model [Eq. (18)] prediction of total NO_xEI as a function of $(1 - y_{f,m})$ at various values of s is also displayed in Fig. 2. The expected trend of increasing total NO_x with s at

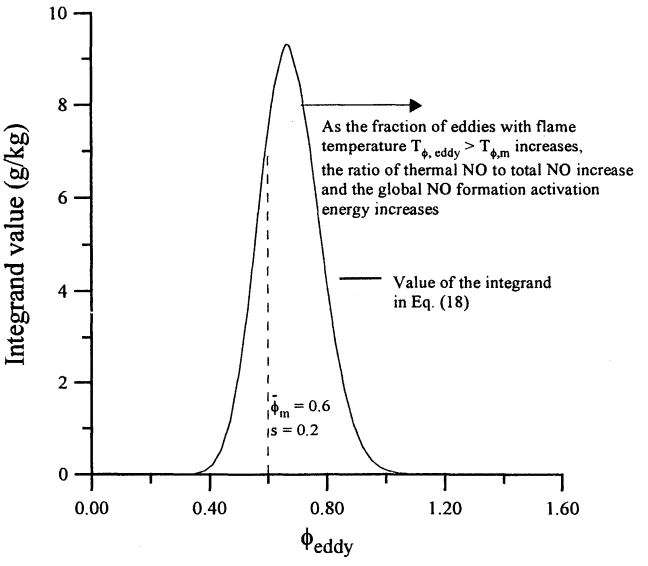

Fig. 8 Graph of the integrand in Eq. (18) for $\bar{\phi}_m = 0.6$ and $s = 0.20$.

$y_{f,m}$ near one is shown. Note that the effect of unmixedness on total NO_x emissions decreases significantly as pilot NO formation becomes more predominant with decreasing $y_{f,m}$. The standard deviation associated with the $s = 0$ case is computed with Eq. (10). The model predicts that s can be increased to approximately 0.15 before total NO_x levels increase above the standard deviation at $y_{f,m} = 1$.

Summary and Conclusions

A CTM was developed for NO_x emissions from an industrial, piloted-LP, natural gas-fired, can combustor (combustor A). The model is preliminary in that no attempt was made to include the fuel/air unmixedness expected for the premixer, and data for only a single geometry (that of combustor A) were available. However, the piloted-LP NO_x model for combustor A includes terms that do account for NO formed in the LP and pilot diffusion flames. CTMs for conventional (diffusion flame) and LP combustor NO_x emissions were modified and applied to the combustor A data.

The individual pilot and preliminary LP flame NO_x models are then combined to formulate a piloted-LP NO_x model that includes a model for fuel/air unmixedness. As a first approximation the CTM for total piloted-LP NO formation is taken as the linear summation of the individual pilot and LP NO_x models. The assumed Gaussian form of the PDF used to model unmixedness is shown to be in agreement with PDFs computed from available experimental data. Furthermore, the model predicts that a practical fuel/air preparation device resulting in an unmixedness (s) of 0.15 will produce an increase in total NO_x levels of about 15% over the ideal case, for conditions typical of those tested in this study. Verifying this result requires independent measurement of unmixedness and is highly desirable.

Acknowledgments

This paper was prepared with the support of the U.S. Department of Energy, Morgantown Energy Technology Center, under cooperative agreement DE-FC21-92MC29061. L. P. Golan and D. Fant of the Advanced Gas Turbine Systems Research Program at the South Carolina Energy R&D Center served as technical monitors. An early version of the paper was presented as ASME 97-GT-206.

References

[1]Barnes, J. C., Mello, J. P., Mellor, A. M., and Malte, P. C., "Preliminary Study of NO_x, CO, and Lean Blowoff in a Piloted-Lean Pre-

mixed Combustor. Part I: Experimental; Part II: Modeling," Technical Meeting, Central States Section, The Combustion Inst., St. Louis, MO, May 1996 (Papers 31 and 32).

[2]Barnes, J. C., and Mellor, A. M., "Quantifying Unmixedness in Lean Premixed Combustors Operating Under High Pressure, Fired Conditions," *Journal of Propulsion and Power*, Vol. 14, No. 6, 1998, pp. 974–980.

[3]Tuttle, J. H., Colket, M. B., Bilger, R. W., and Mellor, A. M., "Characteristic Times for Combustion and Pollutant Formation in Spray Combustion," *16th Symposium (International) on Combustion*, The Combustion Inst., Pittsburgh, PA, 1977, pp. 209–219.

[4]Newberry, D. M., and Mellor, A. M., "Semiempirical Correlations of NO_x Emissions from Utility Combustion Turbines with Inert Injection," *Journal of Propulsion and Power*, Vol. 12, No. 3, 1996, pp. 527–533.

[5]Tuttle, J. H., Shisler, R. A., and Mellor, A. M., "Investigation of Liquid Fueled Turbulent Diffusion Flames," *Combustion Science and Technology*, Vol. 14, No. 4–6, 1976, pp. 229–242.

[6]Mellor, A. M., and Washam, R. M., "Characteristic Time Correlations of Pollutant Emissions from an Annular Gas Turbine Combustor," *Journal of Energy*, Vol. 3, No. 4, 1979, pp. 250–253.

[7]Lightman, A. J., and Magill, P. D., "Velocity Measurements in Confined Dual Coaxial Jets Behind an Axisymmetric Bluff Body: Isothermal and Combusting Flows," U.S. Air Force Wright Aeronautical Labs., TR-81-2018, April 1981.

[8]Roquemore, W. M., and Britton, R. L., "Investigation of the Dynamic Behavior of a Bluff Body Diffusion Flame Using Flame Emission," AIAA Paper 82-0178, Jan. 1982.

[9]Magruder, T. D., McDonald, J. P., Mellor, A. M., Tonouchi, J. H., Nicol, D. G., and Malte, P. C., "Engineering Analysis for Lean Premixed Combustor Design," AIAA Paper 95-3136, July 1995.

[10]Nicol, D. G. (1995), "A Chemical Kinetic and Numerical Study of NO_x and Pollutant Formation in Low-Emission Combustion," Ph.D. Dissertation, Dept. of Mechanical Engineering, Univ. of Washington, Seattle, WA, 1995.

[11]Barnes, J. C., "Characteristic Time Models for Gas Fired, Piloted-Lean Premixed Combustors," M.S. Thesis, Dept. of Mechanical Engineering, Vanderbilt Univ., Nashville, TN, 1996.

[12]Plee, S. L., and Mellor, A. M., "Characteristic Time Model Prediction of NO_x in Prevaporizing/Premixing Combustors," Progress Report from Purdue Univ. to Detroit Diesel Allison Div., Indianapolis, IN, and GM Research Labs., General Motors Corp., Warren, MI, June 1977.

[13]Razdan, M. K., McLeroy, J. T., and Weaver, W. E., "Retrofittable Dry Low Emissions Combustor for 501-K Industrial Gas Turbine Engines," American Society of Mechanical Engineers, Paper 94-GT-439, June 1994.

[14]Fric, T. F., "Effects of Fuel-Air Unmixedness on NO_x Emissions," *Journal of Propulsion and Power*, Vol. 9, No. 5, 1993, pp. 708–713.

[15]Gulati, A., and Warren, R. E., "NO_2-Based Laser-Induced Fluorescence Technique to Measure Cold-Flow Mixing," *Journal of Propulsion and Power*, Vol. 10, No. 1, 1994, pp. 54–61.

[16]Mikus, T., and Heywood, J. B. (1971), "The Automotive Gas Turbine and Nitric Oxide Emissions," *Combustion Science and Technology*, Vol. 4, No. 4, 1971, pp. 149–158.

[17]Fletcher, R. S., and Heywood, J. B., "A Model for Nitric Oxide Emissions from Aircraft Gas Turbine Engines," AIAA Paper 71-123, Jan. 1971.

[18]Mongia, R., Tomita, E., Hsu, F., Talbot, L., and Dibble, R., "Optical Probe for In-Situ Measurements of Air-to-Fuel Ratio in Low Emission Engines," AIAA Paper 96-0174, Jan. 1996.

[19]McDonald, J. P., and Mellor, A. M., "Design of Inlet Conditions for High Pressure NO_x Measurements in Lean Premixed Combustors," American Society of Mechanical Engineers, Paper 95-GT-136, June 1995.

[20]Hautman, D. J., Haas, R. J., and Chiapetta, L., "Transverse Gaseous Injection into Subsonic Air Flows," AIAA Paper 91-0576, Jan. 1991.

[21]Hautman, D. J., "Emissions Performance of a Ramburner Sector of a Mach 5 Combined-Cycle Engine," American Society of Mechanical Engineers, Paper 95-GT-163, June 1995.

[22]Snyder, T. S., Rosfjord, T. J., McVey, J. B., and Chiappetta, L. M., "Comparison of Liquid Fuel/Air Mixing and NO_x Emissions for a Tangential Entry Nozzle," American Society of Mechanical Engineers, Paper 94-GT-283, June 1994.

Tactical Missile Propulsion

G.E. Jensen and David W. Netzer, editors

With contributions from the leading researchers and scientists in the field, this new volume is a compendium of the latest advances in tactical missile propulsion. The objectives of the book are to provide today's designer with a summary of the advances in potential propulsion systems as well as provide a discussion of major design and selection considerations. Authors were chosen for their demonstrated knowledge of and excellence in their respective fields to ensure a complete and up-to-date summary of the latest research and developments.

CONTENTS:

Introduction • Tactical Missile Design Concepts • Liquid Rockets • Solid Rocket Motor Design • Solid Propellant Grain Structural Behavior and Service Life Prediction • Nozzle Design • Solid Rocket Case Design • Solid Rocket Plumes • Insensitive Munitions for Tactical Motors Rocket • Gas Turbines • Liquid Fueled Ramjets Engines • Ducted Rockets • Solid Fuel Ramjets • High Mach Number Applications: Combined Cycles

1996, 529 pp, illus, Hardback
ISBN 1-56347-118-3
AIAA Members $89.95
List Price $104.95
Order #: V-170(945)

AIAA

American Institute of Aeronautics and Astronautics
Publications Customer Service, 9 Jay Gould Ct., P.O. Box 753, Waldorf, MD 20604
Fax 301/843-0159 Phone 800/682-2422 8 a.m. –5 p.m. Eastern

CA and VA residents add applicable sales tax. For shipping and handling add $4.75 for 1–4 books (call for rates for higher quantities). All individual orders, including U.S., Canadian, and foreign, must be prepaid by personal or company check, traveler's check, international money order, or credit card (VISA, MasterCard, American Express, or Diners Club). All checks must be made payable to AIAA in U.S. dollars, drawn on a U.S. bank. Orders from libraries, corporations, government agencies, and university and college bookstores must be accompanied by an authorized purchase order. All other bookstore orders must be prepaid. Please allow 4 weeks for delivery. Prices are subject to change without notice. Returns in sellable condition will be accepted within 30 days. Sorry, we can not accept returns of case studies, conference proceedings, sale items, or software (unless defective). Non-U.S. residents are responsible for payment of any taxes required by their government.